 doi:10.20944/preprints202106.0349.v1

Myofibril and mitochondrial area changes in type I and II fibers following 10 weeks of resistance training in previously untrained men

Bradley A. Ruple[1†], Joshua S. Godwin[1†], Paulo. H. C. Mesquita[1], Shelby C. Osburn[1], Casey L. Sexton[1], Morgan A. Smith[1], Jeremy C. Ogletree[1], Michael D. Goodlett[2,3], Joseph L. Edison[2,3], Arny A. Ferrando[4], Andrew D. Fruge[5], Andreas N. Kavazis[1], Kaelin C. Young[1,3], Michael D. Roberts[1,3*]

Affiliations: [1]School of Kinesiology, Auburn University, Auburn, AL, USA; [2]Athletics Department, Auburn University, Auburn, AL, USA; [3]Edward Via College of Osteopathic Medicine, Auburn, AL, USA; [4]Department of Geriatrics, Donald W. Reynolds Institute on Aging, University of Arkansas for Medical Sciences, Little Rock, AK, USA; [†]indicates co-first authors; [5]Department of Nutrition, Dietetics and Hospitality Management, Auburn University, Auburn, AL, USA

Sources of Support: Funding for participant compensation and assays were provided through laboratory gift donations provided to M.D.R.

Conflicts of interest: MDR receives laboratory funding from various industry sources in the form of fixed-priced contracts or laboratory gifts. MDR has also been financially compensated from various industry entities for consultation work regarding scientific presentations and/or various scientific writing endeavors in accordance with Auburn University's Research Compliance and Ethics Guidelines. In relation to the current study, however, none of the authors has financial or other conflicts of interest to report.

Word Count (abstract+body, no references): 6943
Number of Figures: 8
Number of Tables: 2

[*]Address correspondence to:
Michael D. Roberts, PhD
Associate Professor, School of Kinesiology
Director, Molecular and Applied Sciences Laboratory
Director, Applied Physiology Laboratory
Auburn University
301 Wire Road, Office 260
Auburn, AL 36849
Phone: 334-844-1925
Fax: 334-944-1467
E-mail: mdr0024@auburn.edu

 doi:10.20944/preprints202106.0349.v1

ABSTRACT

Resistance training increases myofiber hypertrophy, but the morphological adaptations that occur within myofibers remain largely unresolved. Fifteen males with minimal training experience (24±4 years, 17.9±1.4 kg/m^2 lean body mass index) performed 10 weeks of conventional, full-body resistance training (2x weekly). Body composition, the radiological density of the vastus lateralis muscle using peripheral quantitative computed tomography (pQCT), and vastus lateralis muscle biopsies were obtained one week prior to and 72 hours following the last training bout. Fiber typing and the quantification of myofibril and mitochondrial areas per fiber were performed using histology/immunohistochemistry (IHC) techniques. Relative myosin heavy chain and actin protein abundances per wet muscle weight as well as citrate synthase (CS) activity assays were also obtained on tissue lysates. Training increased whole-body lean mass, mid-thigh muscle cross-sectional area, various strength metrics, and mean and type II fiber cross sectional areas (fCSA) ($p<0.05$). Myofibril areas in type I or II fibers were not altered with training, suggesting a proportional expansion with fCSA increases. Relative myosin heavy chain and actin protein abundances also did not change with training. IHC indicated training increased mitochondrial areas in both fiber types ($p=0.018$). However, CS activity levels remained unaltered with training. Interestingly, although pQCT-derived muscle density increased with training ($p=0.036$), suggestive of myofibril packing, a positive association existed between training-induced changes in this metric and changes in type I+II myofibril areas ($r=0.600$, $p=0.018$). Shorter-term resistance training seemingly involves a proportional expansion of myofibrils and an accelerated expansion of mitochondria in type I and II fibers. Additionally, histological and biochemical techniques should be viewed independently from one another given the lack of agreement between the variables assessed herein. Finally, the pQCT may be a viable tool to non-invasively track morphological changes in muscle tissue.

KEYWORDS: myofibrils; mitochondria; resistance training

 doi:10.20944/preprints202106.0349.v1

INTRODUCTION

Resistance training increases variables associated with muscle hypertrophy and strength (reviewed in [1]). However, the morphological adaptations that occur in myofibers during resistance training have not been fully elucidated [2,3]. It is generally assumed that increases in muscle fiber cross-sectional area (fCSA) with weeks to months of training coincides with the proportional expansion of all intracellular components (i.e., conventional hypertrophy). However, researchers have utilized elegant techniques to show that training-induced hypertrophy likely occurs one of three ways [4]. First, there are reports to support the conventional hypertrophy model [5-7]. There is also evidence to suggest the expansion of non-myofibril components predominate during muscle fiber hypertrophy [8,9], and this has been termed sarcoplasmic hypertrophy [4]. Lastly, there is evidence to suggest the expansion of myofibrils predominate during muscle fiber hypertrophy with long-term resistance training [10,11], and this has been termed myofibril packing. There are also conflicting reports regarding how mitochondrial volume is affected with resistance training [12]. In this regard, some studies suggest mitochondrial volume increases in proportion with hypertrophy [13-15], while other studies have reported that a dilution in mitochondrial volume occurs with training [8,9,16-18]. Additionally, a surrogate marker of mitochondrial volume (citrate synthase (CS) activity) has been reported to increase following 12 weeks of resistance training, suggesting increases in mitochondrial volume occurred more rapidly than increases in myofiber growth [19].

Transmission electron microscopy (TEM) has been generally viewed as the gold standard in examining the intra-myocellular adaptations to exercise training. While TEM imaging studies provide indispensable information, the laboratory methods are laborious and require specialized equipment to perform. Furthermore, TEM only provides morphology data on small portions of one or two myofibers within each field of view, and experimental artifacts (e.g., organelle expansion or shrinkage) can occur during sample preparation [20].
Histology/immunohistochemistry (IHC) provides an alternative experimental tool to study myofiber adaptations during resistance training, albeit it is limited in magnification and is, therefore, not comparable to TEM in terms of providing structural characteristics about organelles (e.g., mitochondrial membrane structure, the spacing of thick and thin filaments within myofibrils, etc.). However, histological/IHC techniques can be used to quantify the space occupied by organelles within myofibers, and this can offer advantages relative to TEM imaging. For example, histology/IHC allows for the sampling of dozens of whole fibers, and this likely provides a more representative milieu relative to partial fiber imaging with TEM. Additionally, histology/IHC samples can be prepared without dehydration and with less stringent fixatives (or no fixatives at all), thus leading to less morphological artifacts. Lastly, histology/IHC allows for muscle fiber type differentiation, whereas TEM does not. In light of the aforementioned, the purpose of the current study was to use phalloidin-actin staining and mitochondrial import receptor subunit TOM20 homolog (TOMM20) IHC to examine how 10 weeks of resistance training affects areas occupied by myofibrils and mitochondria, respectively, in type I and type II fibers. Biochemical methods that have been used to indirectly assess myofibril and mitochondrial densities were also performed to examine: i) if these variables were altered with training, and ii) if data yielded from these techniques were associated with data generated through phalloidin-actin staining and TOMM20 IHC. Finally, the radiological density of the vastus lateralis muscle was obtained prior to and following training and compared to data yielded from the aforementioned techniques given that this metric has been suggested to largely represent myofibril protein density of muscle tissue [6,21,22]. Based on some of the prior

Preprints (www.preprints.org) | NOT PEER-REVIEWED | Posted: 14 June 2021 doi:10.20944/preprints202106.0349.v1

literature, we hypothesized that: i) areas occupied by myofibrils and mitochondria would disproportionately change relative to changes in fiber area (i.e., muscle fibers would demonstrate sarcoplasmic hypertrophy, ii) indirect measures (i.e., relative myosin heavy chain abundance and CS activity levels) would not be significantly associated with histological variables, and iii) training-induced changes in pQCT-determined muscle density would not be significantly associated with changes in muscle fiber myofibril areas.

RESULTS

General training adaptations

Table 2 contains general training adaptations for the 15 participants. Training significantly increased whole-body LSTM according to DXA, mid-thigh muscle cross-sectional area according to pQCT, mean and type II fCSA according to IHC images obtained using the 10x objective, estimated 1RM leg press, and estimated 1RM deadlift. Training did not increase type I fCSA according to IHC images obtained using the 10x objective. Regarding these IHC data, 56±13 type I and 92±35 type II fibers were quantified at PRE, and 48±19 type I and 81±25 type II fibers were quantified at POST.

Table 1. General training adaptations

Variable (units)	Time	Values (n=15)	p-value
DXA LSTM (kg)	PRE POST	56.4±6.7 58.4±6.8	<0.001
Mid-thigh mCSA (cm^2)	PRE POST	145±21 162±20	<0.001
Type I fCSA (μm^2)	PRE POST	4655±1112 5092±1138	0.103
Type II fCSA (μm^2)	PRE POST	5410±1507 6561±1520	0.007
Mean fCSA (μm^2)	PRE POST	5105±1291 6024±1238	0.013
Est. 1RM leg press (kg)	PRE POST	157±54 231±71	<0.001
Est. 1RM deadlift (kg)	PRE POST	105±23 141±24	<0.001

Legend: All data presented as mean ± standard deviation values.

Although self-reported dietary data were not a primary outcome of this investigation, they are provided here for reference. Participants reported consuming more calories per day at POST versus PRE (2152±842 kcal/d versus 1606±526 kcal/d, p=0.028) and more protein per day at POST versus PRE (111±43 g/d versus 79±35 g/d, p=0.016). Thus, the positive training adaptations (e.g., increases in whole body LSTM, mid-thigh mCSA, strength) may have been the combination of progressive overload as well as increases in calories and protein consumed per day.

Changes in type I and II fiber myofibril areas

The image in Fig. 1a demonstrates how myofibril areas in type I and II fibers were quantified as described in the methods section. Data in Fig. 1b indicate that training did not significantly affect myofibril areas in type I or II fibers (training p=0.243, fiber type x training interaction

Preprints (www.preprints.org) | NOT PEER-REVIEWED | Posted: 14 June 2021 doi:10.20944/preprints202106.0349.v1

p=0.418; post hoc analysis within-fibers were not performed). However, there was a fiber effect, where myofibrils occupied more intracellular space in type II versus type I fibers (p=0.033). Regarding these histology data, 11±4 whole type I and 16±6 whole type II fibers were quantified at PRE, and 8±4 whole type I and 13±4 whole type II fibers were quantified at POST.

Figure 1. Type I and II fiber myofibril areas with training

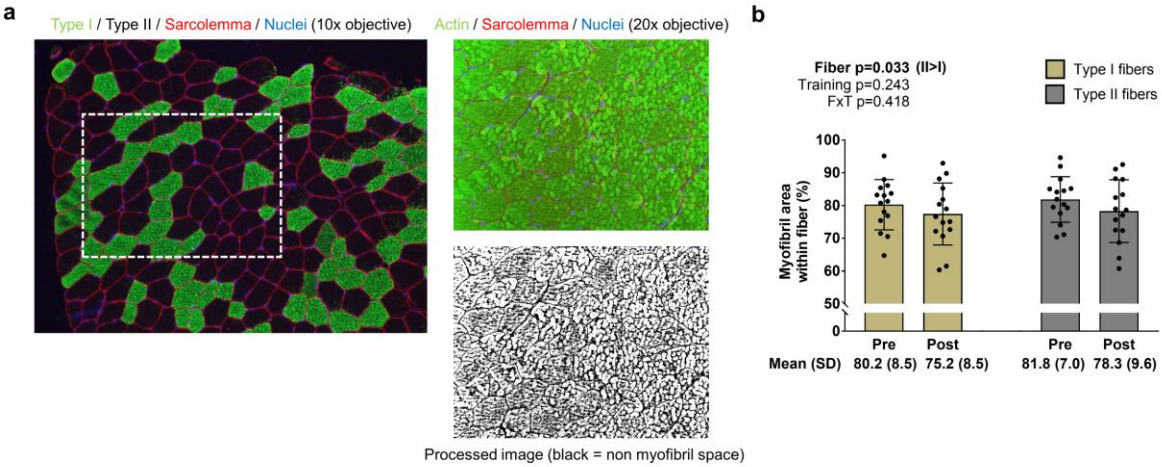

Legend: The figure in panel a is from IHC and phalloidin-actin staining; specifically, this figure demonstrates how myofibril areas were quantified using 20x images, and cross-referenced to fiber type from 10x images of serial sections. Panel b shows how training affected myofibril areas in type I and II fibers. Bar graph data are presented as means ± standard deviation values, and individual participant data are overlaid. n=15 participants. Abbreviation: FxT, fiber x training interaction.

Changes in type I and II fiber mitochondrial areas

Validation experiments using Western blotting show the presence of one sole band ~15 kD in all rat and human muscle samples, and the absence of said band in red blood cell lysates (Fig. 2a); notably, band densities were greater in rat soleus versus plantaris muscle lysates. Regarding IHC validation, rat soleus myofibers (which contain >90% type I fibers) visually present a higher enrichment of TOMM20 compared to rat plantaris myofibers (which contain >90% type I fibers) (Fig. 2b). The image in Fig. 2c demonstrates how mitochondrial areas in type I and II fibers were quantified from our participants that resistance trained using thresholding and fiber tracing techniques. Data in Fig. 2d show that no fiber x training interaction existed for mitochondrial areas (p=0.182). However, there was a fiber effect where mitochondria occupied more intracellular space in type I versus type II fibers (p=0.006). Additionally, there was a training effect where mitochondrial area was greater at POST versus PRE (p=0.018). Regarding these IHC data, 10±3 whole type I and 15±8 whole type II fibers were quantified at PRE, and 9±3 whole type I and 12±5 whole type II fibers were quantified at POST.

Preprints (www.preprints.org) | NOT PEER-REVIEWED | Posted: 14 June 2021 doi:10.20944/preprints202106.0349.v1

Figure 2. Type I and II fiber mitochondrial areas with training

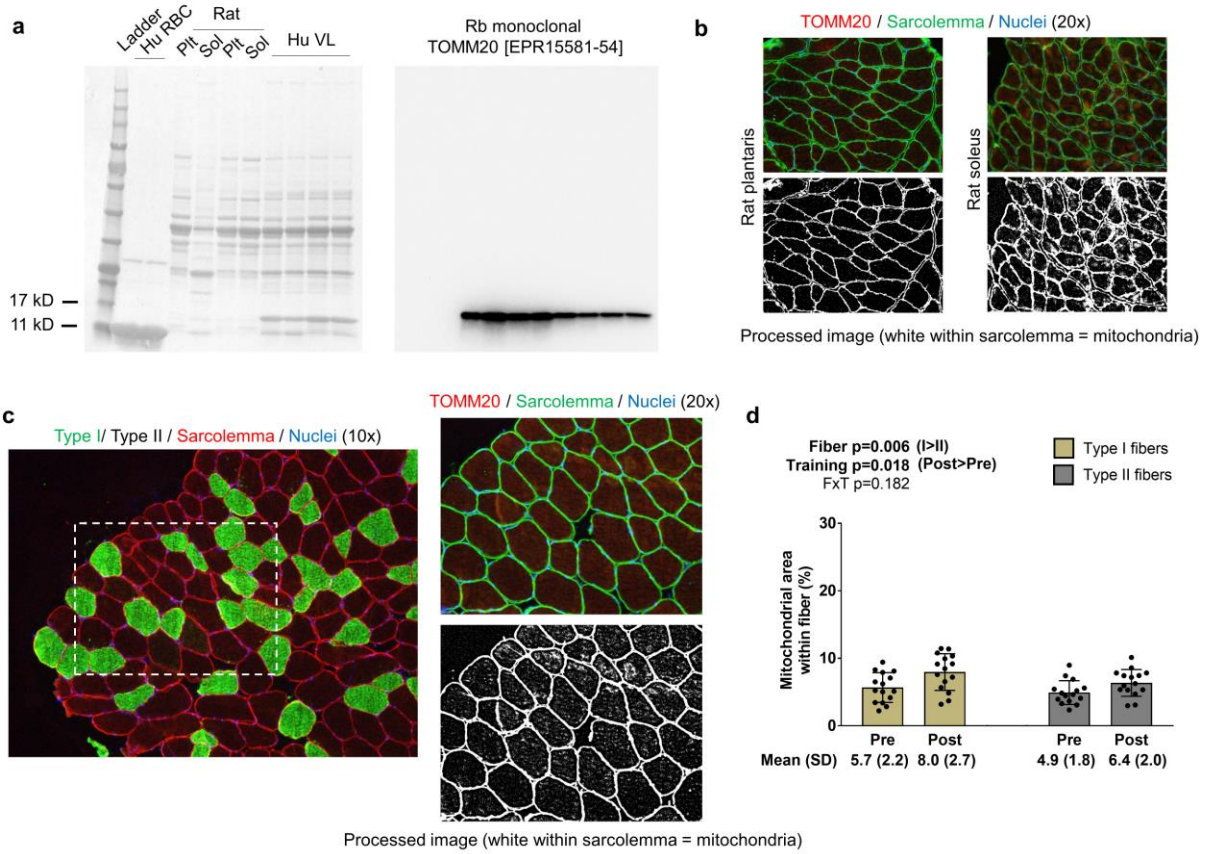

Legend: Panel a shows Western blotting validation results regarding the veracity of the TOMM20 antibody. The left inset is the Ponceau stain of human red blood cells (Hu RBC), rat plantaris (Plt) and soleus (Sol) lysates, and human vastus lateralis muscle (Hu VL). The right inset contains results from Western blotting. Panel b shows IHC validation results from rat Plt and Sol muscles (20x images). Panel c shows IHC and TOMM20 staining from our human participants; specifically, this figure demonstrates how mitochondrial areas were quantified using 20x images, and cross-referenced to fiber type from 10x images of serial sections. Panel b shows how training affected mitochondrial areas in type I and II fibers. Bar graph data are presented as means ± standard deviation values, and individual participant data are overlaid. n=15 participants. Abbreviation: FxT, fiber x training interaction.

Relationships between myonuclear domain and fCSA sizes versus myofibril areas

Data in Fig. 3 show associations between myonuclear domain and fCSA versus myofibril areas in type I and II fibers. No significant associations existed between the following variables: i) change in type I fCSA from PRE to POST and change in type I fiber myofibril area from PRE to POST (Fig. 3a), ii) change in type II fCSA from PRE to POST and change in type II fiber myofibril area from PRE to POST (Fig. 3b), iii) change in type I fiber myonuclear domain size from PRE to POST and change in type I fiber myofibril area from PRE to POST (Fig. 3c), and iv) change in type II fiber myonuclear domain size from PRE to POST and change in type II fiber myofibril area from PRE to POST (Fig. 3d).

Preprints (www.preprints.org) | NOT PEER-REVIEWED | Posted: 14 June 2021 doi:10.20944/preprints202106.0349.v1

Figure 3. Relationships between myonuclear domain and fCSA sizes versus myofibril area

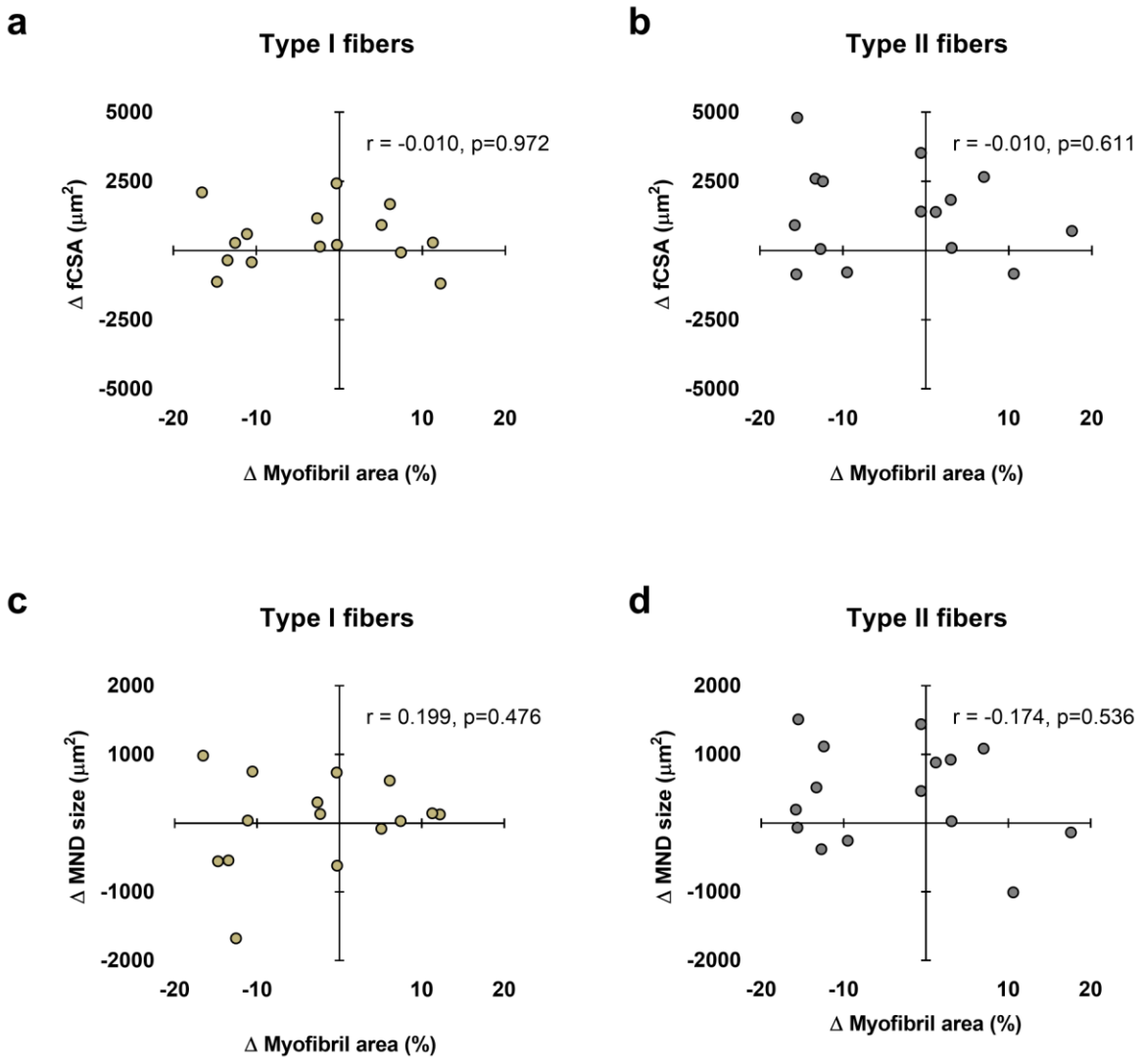

Legend: These plots demonstrate the relationships between changes in type I and II fiber cross-sectional area (fCSA) versus change in myofibril area (panels a and b, respectively), as well as the change in type I and II myonuclear domain (MND) sizes versus change in myofibril area (panels c and d, respectively). n=15 participants in each panel.

Relationships between myonuclear domain and fCSA sizes versus mitochondrial areas
Data in Fig. 4 show associations between myonuclear domain and fCSA versus mitochondrial areas in type I and II fibers. No significant association existed between the change in type I fCSA from PRE to POST and change in type I fiber mitochondrial area from PRE to POST (Fig. 4a). A moderate negative correlation, which trended, existed for change in type II fCSA from PRE to POST and change in type II fiber mitochondrial area from PRE to POST (Fig. 4b). A significant negative correlation existed between the change type I fiber myonuclear domain size

Preprints (www.preprints.org) | NOT PEER-REVIEWED | Posted: 14 June 2021 doi:10.20944/preprints202106.0349.v1

from PRE to POST and change in type I fiber mitochondrial area from PRE to POST (Fig. 4c). No significant association existed between the change in type II fiber myonuclear domain size from PRE to POST and change in type II fiber mitochondrial area from PRE to POST (Fig. 4d). Notably, two subjects were removed from data in panel c due to poor DAPI staining, and one subject was removed from panel d for the same reason.

Figure 4. Relationships between myonuclear domain and fCSA sizes versus mitochondrial area

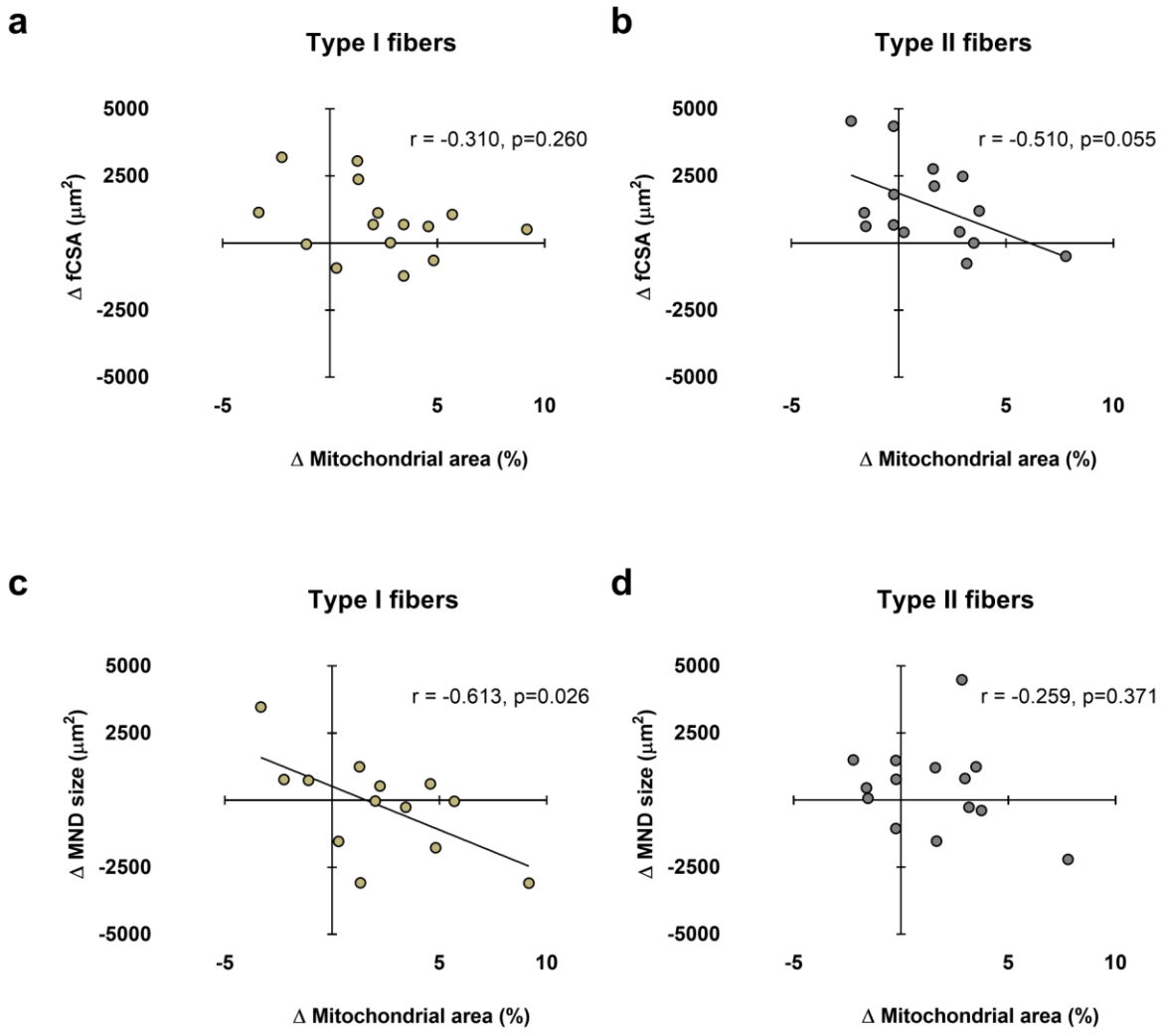

Legend: These plots demonstrate the relationships between changes in type I and II fiber cross-sectional area (fCSA) versus change in mitochondrial area (panels a and b, respectively), as well as the changes in type I and II myonuclear domain (MND) sizes versus change in mitochondrial area (panels c and d, respectively). n=13-15 participants in each panel.

Preprints (www.preprints.org) | NOT PEER-REVIEWED | Posted: 14 June 2021 doi:10.20944/preprints202106.0349.v1

Radiological density data of the vastus lateralis
The image in Fig. 5a shows the mid-thigh region of interest that was quantified for muscle tissue density using the pQCT and associated analysis software. Data in Fig. 5b show that training significantly increased muscle tissue density in this region (p=0.036).

Figure 5. Radiological density data of the vastus lateralis

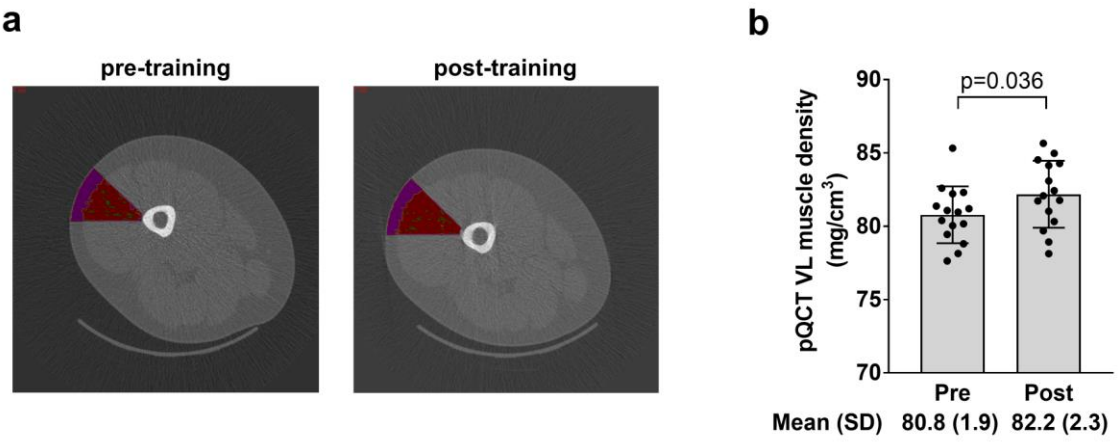

Legend: The figure in panel a demonstrates the region of interest drawn over the mid-thigh scan to extrapolate tissue density in a portion of the vastus lateralis (where the biopsy occurred). Panel b shows how training affected vastus lateralis (VL) density. Bar graph data are presented as means ± standard deviation (SD) values, and individual participant data are overlaid. n=15 participants.

Electrophoresis and CS activity data
The image in Fig. 6a demonstrates how myosin heavy chain and actin bands were quantified as described in the methods section. Data in Fig. 6b/c/d show that training did not significantly affect myosin heavy chain or actin band densities (p=0.969 and 0.347, respectively), sarcoplasmic protein concentrations (p=0.092), or CS activity (p=0.428). Notably, one subject was removed from data in panels c and d due to potential contamination of the sarcoplasmic protein pool.

Preprints (www.preprints.org) | NOT PEER-REVIEWED | Posted: 14 June 2021 doi:10.20944/preprints202106.0349.v1

Figure 6. Electrophoresis, sarcoplasmic protein, and CS activity data

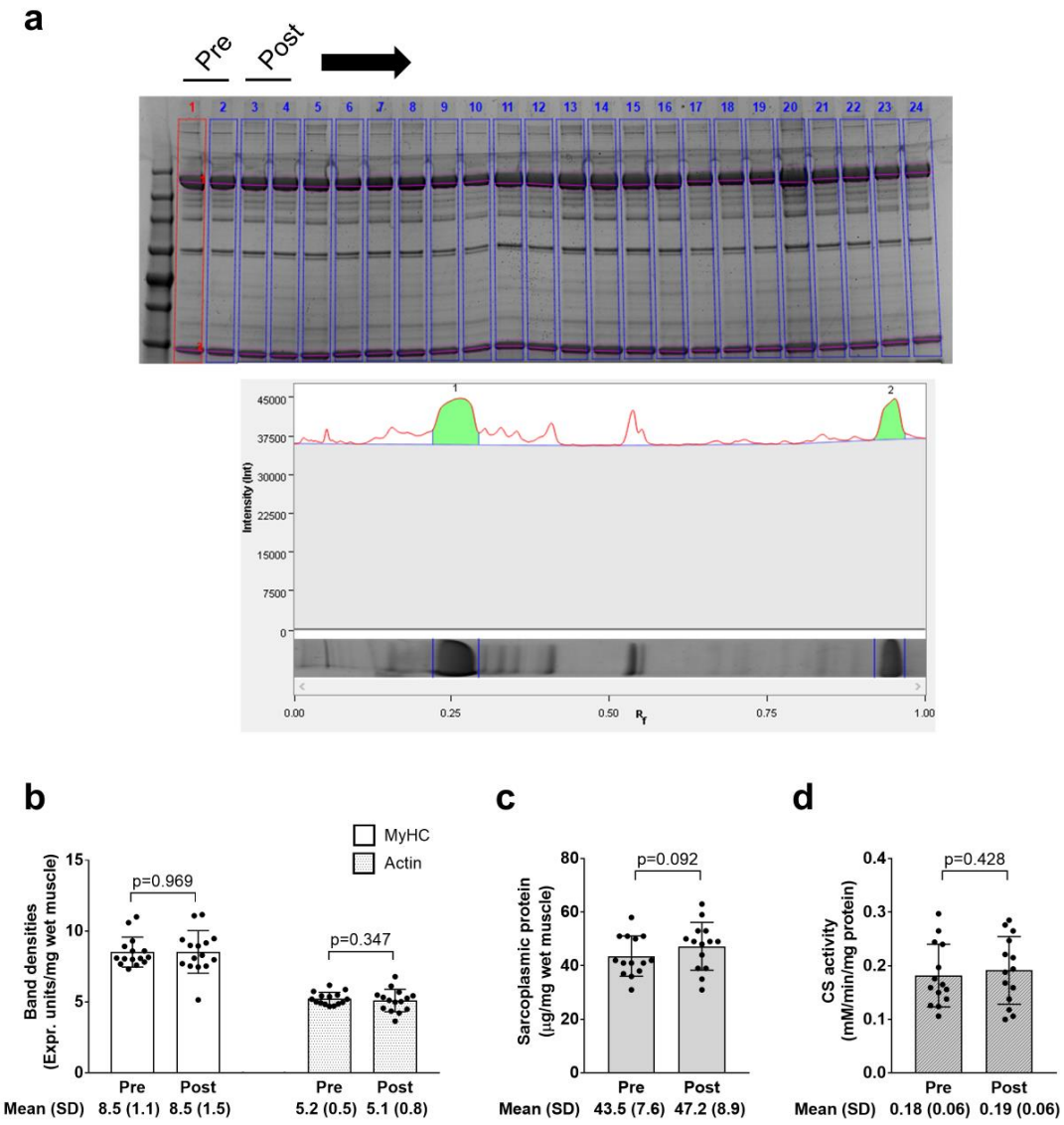

Legend: The figure in panel a is from SDS-PAGE; specifically, this figure demonstrates how the relative densities of myosin heavy chain and actin (lane 1 in this image) were quantified using band densitometry. Panel b shows how training affected relative myosin heavy chain (MyHC) and actin protein content per milligram wet muscle. Panel c shows how training affected sarcoplasmic protein concentrations per milligram wet muscle. Panel d shows how training affected CS activity levels, a surrogate of mitochondrial volume. Bar graph data are presented as means ± standard deviation values, and individual participant data are overlaid. n=14 participants in the CS activity and sarcoplasmic protein panels, and n=15 participants in other panels.

Associations between histological, biochemical, and radiological techniques

Data in Fig. 7 show associations between the various techniques. In short, no significant associations existed between the following variables: i) change in tissue myosin heavy chain

Preprints (www.preprints.org) | NOT PEER-REVIEWED | Posted: 14 June 2021 doi:10.20944/preprints202106.0349.v1

band density from PRE to POST and change in type I+II fiber myofibril area from PRE to POST (Fig. 7a), and ii) change in tissue CS activity from PRE to POST and change in type I+II fiber mitochondrial area from PRE to POST (Fig. 7b). Interestingly, there was a significant positive association between the change in mean (type I+II) fiber myofibril areas from PRE to POST and change in pQCT-derived vastus lateralis muscle density from PRE to POST (Fig. 7c).

Figure 7. Associations between histology, biochemical, and radiological techniques

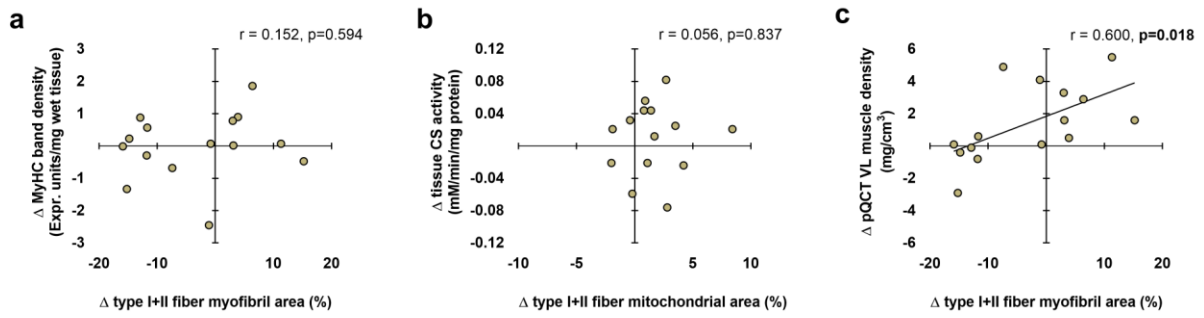

Legend: These plots demonstrate the relationships between changes in type I+II fiber myofibril area versus change in tissue myosin heavy chain band density (panel a), changes in type I+II mitochondrial area versus change in tissue CS activity (panel b), and changes in type I+II fiber myofibril area versus change in tissue pQCT-derived vastus lateralis (VL) muscle density (panel c). n=15 participants in each panel.

DISCUSSION

Recent publications have discussed how resistance training may affect morphological adaptations in myofibers [2,4]. Many investigations in this area utilized TEM or biochemical methods to draw conclusions [5,6,8,9,16-19,23]. However, TEM has limitations related to tissue processing and spatial sampling as discussed prior. Additionally, biochemical methods provide surrogate measures of spatial attributes in myofibers. Thus, we allocated histological and IHC techniques to examine how 10 weeks of resistance training affects myofibril and mitochondrial areas, respectively, in type I and II fibers. In summary, our data suggest myofibril areas within fibers proportionally expanded with increases in fCSA regardless of fiber type. Additionally, we observed increases in mitochondrial areas within myofibers, suggesting resistance training promoted mitochondrial expansion that outpaced increases in fiber size. These findings are discussed in greater detail below.

We have championed the notion that sarcoplasmic hypertrophy may be a resistance training adaptation [4]. Likewise, we have posited that resistance training may cause a mitochondrial volume dilution effect through the disproportionate increase in muscle fiber size relative to mitochondrial expansion with resistance training [12]. The current findings contradict these hypotheses as well as select literature suggesting sarcoplasmic hypertrophy [8,9] and/or mitochondrial volume dilution [5,8,16,17] occurs with weeks to months of resistance training. There are reasons as to why our findings do not agree with these prior reports. First, it should be noted that participants in the two prior studies supporting the sarcoplasmic hypertrophy model

were well trained, and the current participants were not. Moreover, participants in the study by Haun and colleagues engaged in an unconventional and very high-volume training paradigm [8], and a majority of the well-trained participants in the study by MacDougall and colleagues were anabolic steroid users. Thus, if sarcoplasmic hypertrophy is indeed a training adaptation, it remains possible that this phenomenon occurs in well-trained individuals who perform very high volume training blocks or in individuals that administer anabolic steroids. Regarding the mitochondrial dilution hypothesis, it is difficult to reconcile why this finding was not replicated herein. However, much of these data have been reliant upon using CS activity as a surrogate marker of mitochondrial volume [12]. Here, we show that a poor association existed when correlating the changes in type I+II fiber TOMM20 area and tissue CS activity. Thus, while the CS activity assay may provide a crude assessment of mitochondrial content in tissue homogenates, it may lack the sensitivity to track changes in mitochondrial volume with exercise training interventions. This point will be further discussed below.

Aside from the aforementioned hypotheses, we have also posited that myofibril density may be directly influenced by either myofiber and/or myonuclear domain sizes [4]. Specifically, we posited that if fCSA or myonuclear domain sizes became too large with resistance training, this might elicit "transcriptional burden" in resident myonuclei and lead to a disproportionate expansion of non-contractile components. This same logic can also be applied to mitochondria, where a rapid enlargement in myonuclear domain size may hamper the ability of myofibers to facilitate mitochondrial expansion. Had these hypotheses been valid, then data in Figs. 4 and 5 would have yielded significant negative associations between either the changes in fCSA or myonuclear domain sizes and the changes in myofibril and/or mitochondrial areas with training. The data in Fig. 4 partially refute our hypothesis given that, in both fiber types, no significant associations were evident. These data suggest conventional hypertrophy, rather than myofibril packing or sarcoplasmic hypertrophy, is the mode through which initial training adaptations occur within a 10-week resistance training period in previously untrained males. However, two moderate negative associations in Fig. 5 seemingly agree with our hypothesis and warrant further discussion. First, the data in Fig. 5b suggest that the change in type II fiber mitochondrial area was generally not as robust in participants experiencing greater type II fiber hypertrophy. The data in Fig. 5c suggest that the change in type I fiber mitochondrial area was generally not as robust in participants experiencing greater increases in type I fiber myonuclear domain size. Both sets of data imply that mitochondrial expansion may be hampered during rapid fiber growth and/or a rapid expansion in the myonuclear domains with resistance training. This makes intuitive sense given that several genes needed for mitochondrial biogenesis and remodeling are expressed from the nuclear genome [24]. It is also possible that rapidly hypertrophying fibers preferentially synthesize other organelles (e.g., myofibrils and the sarcoplasmic reticulum) prior to mitochondrial expansion during periods of resistance training. Given that these data are limited to correlations, more research is needed to explore the potential relationships between the expansion of the myonuclear domain and mitochondria.

In spite of the aforementioned histological and electrophoresis data suggesting myofibril density remains unaltered with training, pQCT-derived vastus lateralis muscle density significantly increased. The radiological density of muscle tissue has been previously used to make inferences about the morphological adaptations that occur within myofibers. For instance, Claassen et al. [6] reported 6 weeks of resistance training increased Hounsfield units of the mid-thigh by ~4-5% in college-aged men. The authors suggested this was due to either an increase in connective tissue density and/or an increase in contractile protein density. We have also

observed that pQCT-derived muscle density significantly increases in older participants following 6-10 weeks of resistance training [22], and explained our data in a similar fashion. One manner to view data from the current study is that inferences made from the pQCT are limited given that our histology and electrophoresis data indicated no change in myofibril density occurred with training. However, the significant positive association between the training-induced changes in type I+II fiber myofibril area and changes in vastus lateralis muscle density do lend credence to pQCT being a viable non-invasive and indirect representation of myofiber protein density. Due to the limited n-sizes herein, however, future research is needed to determine the validity of this relationship.

Also notable is the lack of agreement between our data yielded from histology/IHC versus data yielded from the allocated biochemical techniques. Specifically, a poor association existed when comparing the training-induced changes in type I+II myofibril area to changes in relative myosin heavy chain protein content (determined by SDS-PAGE) with training. As mentioned above, a poor association also existed when comparing changes in type I+II mitochondrial area to changes in CS activity levels with training. The latter data are provocative given that CS activity has been widely used as a surrogate marker for mitochondrial volume [12], and this relationship was initially established in 16 males by comparing data yielded from the CS activity assay to TEM data [25]. Although it is difficult to reconcile why these methods did not agree, it is notable that we and others have observed similar outcomes when comparing different techniques used to ascertain muscle hypertrophy [1]. Specifically, fCSA increases with resistance training seldom correlate with data yielded from imaging techniques (e.g., muscle thickness of the vastus lateralis, or leg LSTM from the DXA). The discordance herein may be due to utilized histological techniques only providing a two-dimensional representation of dozens of myofibers, whereas the biochemical techniques assayed characteristics of ~20 mg of tissue. Nonetheless, these findings reiterate the notion that data yielded from histological and biochemical techniques may not always agree with one another. Moreover, given the TEM typically samples less myofibers than what were sampled with histology techniques utilized herein, the validity in relating CS activity data to mitochondrial volume should be reappraised when tracking changes during exercise interventions.

Other interesting findings were evident herein. First, our myofibril data generated through phalloidin-actin staining agree with prior TEM data suggesting myofibrils occupy ~80% of the intracellular space within myofibers [9,23]. Moreover, these data show that more of the intracellular space is occupied by myofibrils in type II versus I fibers, which also agrees with prior TEM data [23]. Our TOMM20 IHC data yielded interesting results in that it showed the space occupied by mitochondria was lower in type II versus type I fibers (i.e., a fiber type effect). Moreover, the percent area occupied by mitochondria was (on average) between 5-6% at PRE, and these data agree with TEM investigations suggesting the mitochondria occupy less than 10% of myofibers in humans [16,23].

Experimental considerations

The current data should be viewed with certain limitations in mind. First, the biopsy data are limited to dozens of myofibers, and to suggest that the results extrapolate to the whole muscle is a bold assumption. Notwithstanding, we maintain histological data likely provide a better representation of the intramuscular milieu than that provided through TEM for the reasons discussed. Another limitation is that the histological techniques employed herein provide two-dimensional data about myofibers. Indeed, this is a larger limitation to most histological

 doi:10.20944/preprints202106.0349.v1

investigations in the field. However, Glancy's group has used three-dimensional scanning electron microscopy techniques to elucidate organelle structures in rodent myofibers [26]. Notably, these researchers have discovered that muscle mitochondria exist as an interconnected reticulum [27]. More recently, this group reported that myofibrils, rather than running parallel to one another, are interconnected to form a lattice/matrix-like structure [28]. Hence, employing similar techniques on muscle specimens obtained prior to and following periods of resistance training will further our understanding regarding how various organelles structurally adapt. Finally, our data are limited to younger males, and it is unknown if these data translate to females or older populations.

Conclusions

In conclusion, myofibril area in type I and II fibers proportionally expand with fCSA increases following 10 weeks of resistance training. Moreover, mitochondrial expansion occurs more rapidly than increases in fCSA, albeit mitochondrial expansion may be dampened in rapidly hypertrophying myofibers. The current data also suggest histological and biochemical techniques used to interrogate resistance training adaptations need to be viewed independently from one another given the lack of agreement between the variables assessed herein. Finally, more research is needed to determine if the pQCT can be used to non-invasively track changes in myofibril density.

MATERIALS AND METHODS

Ethics approval and participant inclusion criteria

All procedures were approved by the Institutional Review Board at Auburn University (Protocol #20-136 MR 2004), and this study conformed to the standards set by the latest revision of the Declaration of Helsinki. Eligible participants had to be male, between the ages of 18-30 years, free from cardio-metabolic diseases (e.g., morbid obesity, type II diabetes, severe hypertension), and free from medical conditions that precluded the collection of muscle biopsies. Additionally, participants could not be current smokers, and could not have recently engaged in full-body resistance training >1 day per week. Interested participants provided verbal and written consent to participate prior to data collection procedures outlined below.

Study design

The following methods sections provide descriptions of strength testing, testing sessions, and resistance training. A summary schematic of the study design is presented in Fig. 8.

Preprints (www.preprints.org) | NOT PEER-REVIEWED | Posted: 14 June 2021 doi:10.20944/preprints202106.0349.v1

Figure 8. Study design

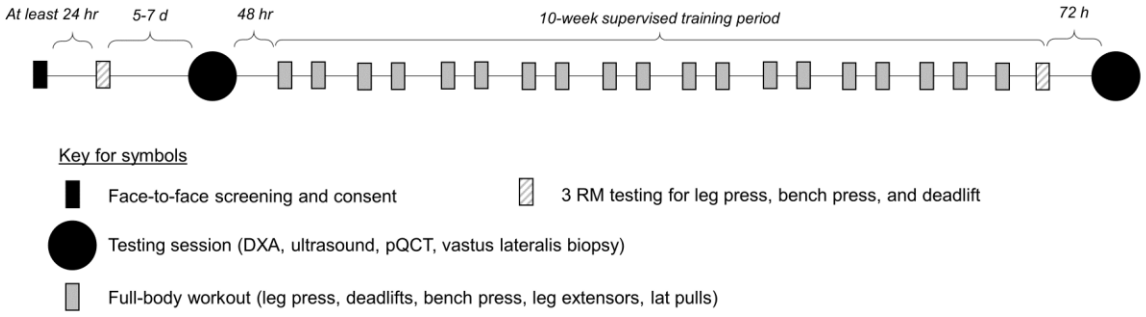

Legend: This figure illustrates the study design.

3RM strength testing

Three repetition maximum (3RM) strength testing for the leg press, bench press and deadlift exercises occurred twice in the study, and obtained values were used to estimate 1RM values according to methods provided by the National Strength and Conditioning Association [29]. The first 3RM session was 5-7 days prior to the PRE testing session, and the second 3RM session occurred as the last workout for the 10-week training period (which was 72 hours prior to the POST testing session). 3RM testing procedures were identical to procedures that we have previously published [30]. Participants were also familiarized with the training during testing of 3RMs. All testing occurred under direct supervision of a technician holding the Certified Strength and Conditioning Specialist Certification (CSCS) from the National Strength and Conditioning Association.

PRE and POST testing sessions

Testing sessions occurred during the morning hours (0600-1100) following an overnight fast. These sessions occurred 3-5 days prior to the 10-week training intervention (PRE), and 72 hours following the last training bout (POST). During these sessions, participants reported to the Auburn University School of Kinesiology wearing casual sports attire (i.e. athletic shirt and shorts, tennis shoes). Additionally, participants were given four-day food logs prior to the PRE and POST testing sessions, and we requested that they return these logs during the visits after having completed the log over two typical weekdays and weekend days. PRE and POST four-day food logs were analyzed using commercially available software (ESHA Food Processor v.11.1, ESHA Research; Salem, OR, USA). Calorie and protein intake data are presented as daily values, which were averaged over the 4-day entries.

Body Composition Assessments. Participants submitted a urine sample (~5 mL) to assess urine specific gravity levels using a handheld refractometer (ATAGO; Bellevue, WA, USA). Notably, all participants possessed values less than 1.020 indicating that they were well hydrated [31]. Height and body mass were then assessed using a digital column scale (Seca 769; Hanover, MD, USA). Participants then underwent a full body dual-energy x-ray absorptiometry (DXA) scan (Lunar Prodigy; GE Corporation, Fairfield, CT, USA) for determination of whole body lean soft tissue mass (LSTM). Quality assurance testing and calibration were performed the morning

Preprints (www.preprints.org) | NOT PEER-REVIEWED | Posted: 14 June 2021 doi:10.20944/preprints202106.0349.v1

of data-collection days to ensure the scanner was operating to manufacturer specification. Scans were analyzed by the same technician using the manufacturer's standardized software. Test-retest reliability using intraclass correlation ($ICC_{3,1}$), standard error of the measurement (SEM), and minimal difference values (MD) were previously determined for LSTM to be 0.99, 0.36, and 0.99 kg, respectively.

Following the DXA scan, a cross-sectional image of the right thigh at 50% of the femur length was acquired using a pQCT scanner (Stratec XCT 3000, Stratec Medical, Pforzheim, Germany). Scans were acquired using a single 2.4 mm slice thickness, a voxel size of 0.4 mm and scanning speed of 20 mm/sec. All images were analyzed for mid-thigh muscle cross-sectional area (mCSA, cm^2) using the pQCT BoneJ plugin freely available through ImageJ analysis software (NIH, Bethesda, MD). All scans were performed and analyzed by the same investigator. Test-retest reliability $ICC_{3,1}$, SEM, and MD values were previously determined for mCSA to be 0.99, 0.84, and 2.32 cm^2, respectively. pQCT images were also analyzed for vastus lateralis radiological density (mg/cm^3) by manually tracing the muscle using this same software. Notably, only skeletal muscle tissue in this region was analyzed for tissue density, as intramuscular and subcutaneous fat was excluded.

Muscle collection. After body composition and mid-thigh assessments, skeletal muscle biopsies were obtained from the right thigh (i.e., vastus lateralis; in the same plane as ultrasound and pQCT assessments) using a 5-gauge needle with suction and sterile procedures. Briefly, participants were instructed to lie in a supine position on an athletic training table. Lidocaine (1%, 1.5 mL) was injected subcutaneously above the skeletal muscle fascia at the collection site. After 5 minutes of allowing the anesthetic to take effect, a small pilot incision was made using a sterile Surgical Blade No. 11 (AD Surgical; Sunnyvale, CA, USA), and the biopsy needle was inserted into the pilot incision just below the fascia. Approximately 50-80 mg of skeletal muscle was removed using a double chop method and applied suction [32]. Following biopsies, tissue was rapidly teased of blood and connective tissue. A portion of the tissue (~10-20 mg) was preserved in freezing media for histology (Tissue-Tek®, Sakura Finetek Inc; Torrence, CA, USA), slow frozen in liquid nitrogen-cooled isopentane, and subsequently stored at -80°C. Another portion of the tissue (~30-50 mg) was placed in pre-labelled foils, flash frozen in liquid nitrogen, and subsequently stored at -80°C until the isolation of myofibrils and other assays described below.

Resistance training

Two days following the PRE testing battery, resistance training commenced. Training occurred two days per week where participants were allowed to train from either 0700-0900 or 1530-1830 on Monday or Tuesday and Wednesday or Thursday of each week. Participants were instructed to not perform other vigorous exercise activities outside of the study.

Prior to beginning each training session, participants were instructed to perform a general warm-up involving 25 jumping jacks, 10 bodyweight squats, and 10 push-ups for 2 rounds. Afterward, participants engaged in exercises that included the leg press, barbell deadlift, bilateral leg extensions, bench press, and a machine pulldown exercise designed to target the elbow flexors and latissimus dorsi muscles. Two warm up sets were allowed which were <50% of the working set. Thereafter, working sets were performed according to the set/repetition scheme shown in Table 1. Participants were recommended to take 2 minutes of rest between each exercise set. However, participants were allowed to proceed to the next exercise without 2

Preprints (www.preprints.org) | NOT PEER-REVIEWED | Posted: 14 June 2021 doi:10.20944/preprints202106.0349.v1

minutes of rest if they felt prepared to execute exercises with appropriate technique. Additionally, if participants desired more than 2 minutes of rest, this was allowed. Training load for each exercise was progressed in a pre-programmed manner according to Table 2. However, participant feedback was also taken into consideration. In this regard, a degree of difficulty (RPE) scale was used during workouts where 0 = "very easy" and 10 = "very hard". After each set for each exercise, RPE was gauged by training staff. If RPE was less than 6, then ~10% additional load was added to the exercise. If RPE was less than 4, then ~20% additional load was added to the exercise. If a set was not completed or RPE was 10, then load was adjusted according to the discretion of the research staff. All training occurred under direct supervision of research staff, and all volume was logged.

Table 2. Resistance training scheme

Week	Day	Set x rep scheme	% initial 1RM
1	M/T W/R	4 x 10 5 x 6	50 56
2	M/T W/R	4 x 10 5 x 6	55 65
3	M/T W/R	4 x 10 5 x 6	60 74
4	M/T W/R	4 x 10 5 x 6	65 84
5*	M/T W/R	4 x 10 5 x 6	50 50
6	M/T W/R	4 x 10 5 x 6	65 84
7	M/T W/R	4 x 10 5 x 6	70 90
8	M/T W/R	4 x 10 5 x 6	75 96
9	M/T W/R	4 x 10 5 x 6	80 98
10	M/T W/R	5 x 6 Post strength test	102 ---

Legend: The set x rep scheme presented above was for five exercises per workout (leg press, bench press, deadlift, leg extension, cable pulldown). Additionally, participants worked out either Monday or Tuesday and Wednesday or Thursday for two workouts per week. Notes: *, indicates deload week.

Analyses of muscle specimens

Isolation of myofibrillar and sarcoplasmic protein fractions. Myofibrillar and sarcoplasmic protein isolations were performed based on our published "MIST" method [33], which was derived from Goldberg's laboratory [34]. Tissue foils were removed from -80ºC, and tissue was crushed on a liquid nitrogen-cooled ceramic mortar with a ceramic pestle. Powdered tissue (~20 mg) was placed in 1.7 mL tubes pre-filled with ice-cold buffer (300 µL; Buffer 1: 25

Preprints (www.preprints.org) | NOT PEER-REVIEWED | Posted: 14 June 2021 doi:10.20944/preprints202106.0349.v1

mM Tris, pH 7.2, 0.5% Triton X-100, protease inhibitors) and weighed using an analytical scale sensitive to 0.0001 g. Samples were homogenized using tight-fitting pestles and centrifuged at 1,500 × g for 10 minutes at 4°C. Supernatants (sarcoplasmic fraction) were collected and placed in new 1.7 mL microtubes on ice. As a wash step, the resultant myofibrillar pellet was resuspended in 300 µL of Buffer 1 and centrifuged at 1,500 × g for 10 min at 4°C. The supernatant was discarded and the myofibrillar pellet was solubilized in 400 µL of ice-cold resuspension buffer (20 mM Tris–HCl, pH 7.2, 100 mM KCl, 20% glycerol, 1 mM DTT, 50 mM spermidine, protease inhibitors). The same day of isolations, sarcoplasmic protein samples were assayed in duplicate for total protein using a commercial BCA assay protocol (Thermo Fisher Scientific, Waltham, MA, USA). The average coefficient of variation (CV) for duplicate readings was 2.3%, and sarcoplasmic protein concentrations were normalized to input muscle weights. Sarcoplasmic protein samples were then stored at -80°C until the CS activity assay described below. The same day of isolations, SDS-PAGE myofibril preps were also made using 10 µL resuspended myofibrils, 65 µL distilled water (diH_2O), and 25 µL 4x Laemmli buffer. These preps were boiled for 5 minutes and stored at -80°C until electrophoresis described below.

Electrophoretic determination of myosin and actin content. The electrophoretic determination of relative myosin and actin content were performed as previously described by our laboratory [5,10,35] and others [34]. Briefly, SDS-PAGE preps (5 µL) were loaded in duplicate on pre-casted gradient (4-15%) SDS-polyacrylamide gels (Bio-Rad Laboratories, Hercules, CA, USA) and subjected to electrophoresis at 200 V for 40 minutes using pre-made 1x SDS-PAGE running buffer (VWR International, Radnor, PA, USA). Following electrophoresis gels were rinsed in diH_2O for 10 minutes, and immersed in Coomassie stain (LabSafe GEL Blue; G-Biosciences; St. Louis, MO, USA) for 1 hour. Thereafter, gels were destained in diH_2O for 2 hours, bright field imaged using a gel documentation system (ChemiDoc; Bio-Rad Laboratories), and band densitometry was performed with a gel documentation system and associated software. Given that a standardized volume from all samples were loaded onto gels, myosin and actin band densities were normalized to input muscle weights for relative expression. Our laboratory has reported that this method yields exceptional sensitivity in detecting 5-25% increases in actin and myosin content [5]. Notably, actin and myosin content were the only two myofibrillar protein targets of interest given that the combination of these proteins make up a majority (~70%) of the myofibrillar protein pool as determined via proteomics [10]. The average coefficient of variation values for all duplicates was 2.3% for myosin heavy chain band densities and 2.5% for actin band densities.

CS activity assay. Sarcoplasmic fractions were batch process-assayed for total protein content using a BCA Protein Assay Kit (Thermo Fisher Scientific; Waltham, MA, USA). Thereafter samples were batch processed for CS activity as previously described [5], and this marker was used as a surrogate for mitochondrial content according to previous literature suggesting CS activity highly correlates with electron micrograph images of mitochondrial content in skeletal muscle ($r=0.84$, $p<0.001$) [25]. The assay utilized is based on the reduction of 5, 50-dithiobis (2-nitrobenzoic acid) (DTNB) at 412 nm (extinction coefficient 13.6 mmol/L/cm) coupled to the reduction of acetyl-CoA by the CS reaction in the presence of oxaloacetate. Briefly, 12.5 µg of whole-tissue sample lysates were added to a mixture composed of 0.125 mol/L Tris-HCl (pH 8.0), 0.03 mmol/L acetyl-CoA, and 0.1 mmol/L DTNB. The reaction was initiated by the addition of 5 µL of 50 mM oxaloacetate and the absorbance change was recorded for one minute. The average coefficient of variation values for all duplicates was less than 10%.

Preprints (www.preprints.org) | NOT PEER-REVIEWED | Posted: 14 June 2021 doi:10.20944/preprints202106.0349.v1

IHC for fiber typing, phalloidin-actin staining, and TOMM20 IHC. Sections from OCT-preserved samples were sectioned at a thickness of 10 µm using a cryotome (Leica Biosystems; Buffalo Grove, IL, USA) and adhered to positively charged histology slides. Slides were then stored at -80ºC until batch processing occurred for procedures described below.

For type I and II fCSA determination, sections were first air-dried at room temperature for 10 minutes, permeabilized for 5 minutes using 0.5% Triton-X in PBS, and blocked with 100% Pierce Super Blocker (Thermo Fisher Scientific) for 25 minutes. Sections were then incubated for 60 minutes with a primary antibody solution containing: i) a base buffer of 1x phosphate buffered saline (PBS), ii) 5% Pierce Super Blocker, iii) 2.5% (1:50 dilution) rabbit anti-dystrophin IgG1 antibody (catalog #: GTX15277; Genetex Inc.; Irvine, CA, USA), and iv) 2.5% (1:50 dilution) mouse anti-myosin I IgG1 (catalog #: A4.951 supernatant; Developmental Studies Hybridoma Bank, Iowa City, IA, USA). Sections were subsequently washed for 5 minutes with PBS and incubated in the dark for 60 minutes with a secondary antibody solution containing: i) a base buffer of 1x PBS, ii) 5% Pierce Super Blocker (Thermo Fisher Scientific), iii) Texas Red-conjugated anti-rabbit IgG (catalog #: TI-1000; Vector Laboratories, Burlingame, CA, USA) and Alexa Fluor 488-conjugated anti-mouse IgG1 (catalog #: A-11001; Thermo Fisher Scientific) (~6.6 µL of all secondary antibodies per 1 mL of blocking solution, or a 1:150 dilution). Sections were then washed for 5 minutes in PBS, air-dried, and mounted with fluorescent media containing 4,6-diamidino-2-phenylindole (DAPI; catalog #: GTX16206; Genetex Inc.). Following mounting, digital images were immediately captured with a fluorescent microscope (Nikon Instruments, Melville, NY, USA) using a 10x objective. Exposure times were 200 milliseconds for FITC, 600 milliseconds for TRITC imaging, and 100 milliseconds for DAPI imaging. This staining method allowed the identification of the sarcolemma (detected by the Texas Red filter), type I fiber green cell bodies (detected by the FITC filter), type II fiber black cell bodies (unlabeled), and myonuclei (detected by the DAPI filter). Standardized measurements of type I, type II, and mean fCSAs were performed using open-sourced software (MyoVision) [36]. A pixel conversion ratio value of 0.964 µm/pixel was used to account for the size and bit-depth of images, and a detection range of detection from 500 to 12,000 μm^2 was used to ensure artifact was removed (e.g., large fibers which may have not been in transverse orientation, or structures between dystrophin stains which were likely small vessels).

For the determination of myofibril area per fiber, F-actin labelling using Alexa Fluor 488-conjugated (AF488) phalloidin was performed according to previous reports [8,37,38]. Briefly, serial sections were air-dried for 10 minutes followed by 10% formalin fixation for 10 minutes. Sections were then washed with PBS for 5 minutes, and blocked with 100% Pierce Super Blocker (Thermo Fisher Scientific) for 25 minutes. After blocking, a pre-diluted commercially-available rabbit anti-dystrophin IgG1 antibody solution (catalog #: GTX15277; Genetex Inc.) and spiked in phalloidin-AF488 (1:35 dilution) was placed on sections in the dark for 30 minutes. Sections were subsequently washed in PBS for 5 minutes and incubated in the dark for 20 minutes with a secondary antibody solution containing Texas Red-conjugated anti-rabbit IgG (catalog #: TI-1000; Vector Laboratories; ~6.6 µL secondary antibody per 1 mL of blocking solution). Sections were washed in PBS for 5 minutes, and air-dried and mounted with fluorescent media containing DAPI (catalog #: GTX16206; Genetex Inc.). Following mounting, digital images were immediately captured with a fluorescent microscope (Nikon Instruments) using a 20x objective. Exposure times were 200 milliseconds for FITC, 800 milliseconds for TRITC imaging, and 100 milliseconds for DAPI imaging. This staining method allowed the

 doi:10.20944/preprints202106.0349.v1

identification of the sarcolemma (Texas Red filter), myofibrils (FITC filter), and myonuclei (DAPI filter). ImageJ (NIH) was used to quantify myofibril area per fiber. Briefly, images were split into RGB channels, and the green channel image was converted to grayscale. The threshold function in imageJ was then used to generate binary black/white images of stained versus unstained portions of fibers. Thereafter, fibers were manually traced using the polygon function, and myofibril areas were provided as a percentage per fiber area. A visual representation of this image analysis is provided in Figure 2 in the results section. Fibers that were quantified in this regard were manually matched to fibers on 10x images to derive myofibril areas for type I and type II fibers. Myonuclei from 20x images were also manually assigned to fibers to extrapolate myofibril-myonuclei relationships.

For the determination of mitochondrial area per fiber, TOMM20 IHC was performed in accordance with a previous report that used TOMM20 IHC to estimate mitochondrial content in colorectal tissue [39]. Briefly, a second set of serial sections were air-dried for 10 minutes. Sections were then washed in PBS for 5 minutes, permeabilized for 20 minutes using 0.5% Triton-X in PBS. Sections were then blocked with 100% Pierce Super Blocker (Thermo Fisher Scientific) for 25 minutes, and subsequently incubated for 60 minutes in a primary antibody solution containing: i) a base buffer of 1x PBS, ii) 5% Pierce Super Blocker, iii) 2.5% (or 1:50 dilution) of a commercially-available rabbit anti-TOMM20 monoclonal IgG antibody (catalog #: ab232589; Abcam; Cambridge, MA, USA), and iv) 2.5% (or 1:50 dilution) of a commercially-available mouse anti-dystrophin IgG1 antibody (MANDRA1 supernatant; Developmental Studies Hybridoma Bank). Sections were then washed for 5 minutes with PBS and incubated in the dark for 60 minutes with a secondary antibody solution containing: i) a base buffer of 1x PBS, ii) 5% Pierce Super Blocker, iii) Texas Red-conjugated anti-rabbit IgG (catalog #: TI-1000; Vector Laboratories) and Alexa Fluor 488-conjugated anti-mouse IgG1 (catalog #: A-11001; Thermo Fisher Scientific) (~6.6 µL of all secondary antibodies per 1 mL of blocking solution, or a 1:150 dilution). Sections were washed for 5 minutes in PBS, air-dried and mounted with fluorescent media containing DAPI (catalog #: GTX16206; Genetex Inc.). Following mounting, digital images were immediately captured with a fluorescent microscope (Nikon Instruments) using the 20x objective. Exposure times were 200 milliseconds for FITC and TRITC, and 10 milliseconds for DAPI imaging. This staining method allowed the identification of the sarcolemma (FITC filter), mitochondria (Texas Red filter), and myonuclei (DAPI filter). ImageJ (NIH) was used to quantify mitochondrial area per fiber as described above for phalloidin-actin staining, and fibers were matched to 10x images for fiber typing. A visual representation of this image analysis is provided in Fig. 3 in the results section.

Notably, we extensively validated the TOMM20 antibody by running Western blots on: i) muscle tissue lysates obtained in the current study, ii) red blood cell lysates (note, red blood cells lack mitochondria making this a negative control), iii) rat plantaris muscle, and iv) rat soleus muscle. Additionally, we performed TOMM20 IHC on rat soleus and plantaris muscle. Assayed rat muscle was banked from a prior study published from our laboratory, where tissue collection was approved by the Auburn University Institutional Animal Care and Use Committee [40]. Outcomes from these validation studies are presented in the results section.

Statistics

Statistical analyses were performed using SPSS (Version 25; IBM SPSS Statistics Software, Chicago, IL, USA). The only dependent variables to be analyzed using two-way ANOVAs were fiber type-specific changes in myofibril and mitochondrial areas. If significant fiber type x

 doi:10.20944/preprints202106.0349.v1

training interactions were observed for either of these two variables, it was decided *a priori* that the model would be decomposed using dependent samples t-tests to examine PRE versus POST for each fiber type, and independent samples t-tests to compare each fiber type at PRE and POST. PRE to POST changes in other dependent variables were analyzed using dependent samples t-tests. Select associations between dependent variables were also analyzed using Pearson correlations. All data in tables and figures are presented as mean ± standard deviation values, and statistical significance was set at $p<0.05$.

ACKNOWLEDGEMENTS

We thank the participants who volunteered to take part in this study. We also thank Dr. Christopher Vann and Dr. Cody Haun for their suggestions regarding IHC analysis.

FUNDING

Funding for participant compensation, assays, and article publishing charges were provided through laboratory donations to M.D.R.

CONFLICTS OF INTEREST

M.D.R. receives laboratory funding from various industry sources in the form of fixed-priced contracts or laboratory gifts. M.D.R. has also been financially compensated from various industry entities for consultation work regarding scientific presentations and/or various scientific writing endeavors in accordance with Auburn University's Research Compliance and Ethics Guidelines. In relation to the current data, however, the authors declare that no conflicts of interest exist.

REFERENCES

1. Haun, C.T.; Vann, C.G.; Roberts, B.M.; Vigotsky, A.D.; Schoenfeld, B.J.; Roberts, M.D. A Critical Evaluation of the Biological Construct Skeletal Muscle Hypertrophy: Size Matters but So Does the Measurement. *Front Physiol* **2019**, *10*, 247, doi:10.3389/fphys.2019.00247.
2. Jorgenson, K.W.; Phillips, S.M.; Hornberger, T.A. Identifying the Structural Adaptations that Drive the Mechanical Load-Induced Growth of Skeletal Muscle: A Scoping Review. *Cells* **2020**, *9*, doi:10.3390/cells9071658.
3. Reggiani, C.; Schiaffino, S. Muscle hypertrophy and muscle strength: dependent or independent variables? A provocative review. *Eur J Transl Myol* **2020**, *30*, 9311, doi:10.4081/ejtm.2020.9311.
4. Roberts, M.D.; Haun, C.T.; Vann, C.G.; Osburn, S.C.; Young, K.C. Sarcoplasmic Hypertrophy in Skeletal Muscle: A Scientific "Unicorn" or Resistance Training Adaptation? *Front Physiol* **2020**, *11*, 816, doi:10.3389/fphys.2020.00816.
5. Roberts, M.D.; Romero, M.A.; Mobley, C.B.; Mumford, P.W.; Roberson, P.A.; Haun, C.T.; Vann, C.G.; Osburn, S.C.; Holmes, H.H.; Greer, R.A., et al. Skeletal muscle mitochondrial volume and myozenin-1 protein differences exist between high versus low anabolic responders to resistance training. *PeerJ* **2018**, *6*, e5338, doi:10.7717/peerj.5338.
6. Claassen, H.; Gerber, C.; Hoppeler, H.; Luthi, J.M.; Vock, P. Muscle filament spacing and short-term heavy-resistance exercise in humans. *J Physiol* **1989**, *409*, 491-495, doi:10.1113/jphysiol.1989.sp017509.
7. Shoepe, T.C.; Stelzer, J.E.; Garner, D.P.; Widrick, J.J. Functional adaptability of muscle fibers to long-term resistance exercise. *Med Sci Sports Exerc* **2003**, *35*, 944-951, doi:10.1249/01.MSS.0000069756.17841.9E.
8. Haun, C.T.; Vann, C.G.; Osburn, S.C.; Mumford, P.W.; Roberson, P.A.; Romero, M.A.; Fox, C.D.; Johnson, C.A.; Parry, H.A.; Kavazis, A.N., et al. Muscle fiber hypertrophy in response to 6 weeks of high-volume resistance training in trained young men is largely attributed to sarcoplasmic hypertrophy. *PLoS One* **2019**, *14*, e0215267, doi:10.1371/journal.pone.0215267.
9. MacDougall, J.D.; Sale, D.G.; Elder, G.C.; Sutton, J.R. Muscle ultrastructural characteristics of elite powerlifters and bodybuilders. *Eur J Appl Physiol Occup Physiol* **1982**, *48*, 117-126, doi:10.1007/BF00421171.
10. Vann, C.G.; Roberson, P.A.; Osburn, S.C.; Mumford, P.W.; Romero, M.A.; Fox, C.D.; Moore, J.H.; Haun, C.T.; Beck, D.T.; Moon, J.R., et al. Skeletal Muscle Myofibrillar Protein Abundance Is Higher in Resistance-Trained Men, and Aging in the Absence of Training May Have an Opposite Effect. *Sports (Basel)* **2020**, *8*, doi:10.3390/sports8010007.
11. D'Antona, G.; Lanfranconi, F.; Pellegrino, M.A.; Brocca, L.; Adami, R.; Rossi, R.; Moro, G.; Miotti, D.; Canepari, M.; Bottinelli, R. Skeletal muscle hypertrophy and structure and function of skeletal muscle fibres in male body builders. *J Physiol* **2006**, *570*, 611-627, doi:10.1113/jphysiol.2005.101642.
12. Parry, H.A.; Roberts, M.D.; Kavazis, A.N. Human Skeletal Muscle Mitochondrial Adaptations Following Resistance Exercise Training. *Int J Sports Med* **2020**, *41*, 349-359, doi:10.1055/a-1121-7851.

13. Porter, C.; Reidy, P.T.; Bhattarai, N.; Sidossis, L.S.; Rasmussen, B.B. Resistance Exercise Training Alters Mitochondrial Function in Human Skeletal Muscle. *Med Sci Sports Exerc* **2015**, *47*, 1922-1931, doi:10.1249/MSS.0000000000000605.
14. Salvadego, D.; Domenis, R.; Lazzer, S.; Porcelli, S.; Rittweger, J.; Rizzo, G.; Mavelli, I.; Simunic, B.; Pisot, R.; Grassi, B. Skeletal muscle oxidative function in vivo and ex vivo in athletes with marked hypertrophy from resistance training. *J Appl Physiol (1985)* **2013**, *114*, 1527-1535, doi:10.1152/japplphysiol.00883.2012.
15. Tesch, P.A.; Thorsson, A.; Colliander, E.B. Effects of eccentric and concentric resistance training on skeletal muscle substrates, enzyme activities and capillary supply. *Acta Physiol Scand* **1990**, *140*, 575-580, doi:10.1111/j.1748-1716.1990.tb09035.x.
16. MacDougall, J.D.; Sale, D.G.; Moroz, J.R.; Elder, G.C.; Sutton, J.R.; Howald, H. Mitochondrial volume density in human skeletal muscle following heavy resistance training. *Med Sci Sports* **1979**, *11*, 164-166.
17. Tesch, P.A.; Komi, P.V.; Hakkinen, K. Enzymatic adaptations consequent to long-term strength training. *Int J Sports Med* **1987**, *8 Suppl 1*, 66-69, doi:10.1055/s-2008-1025706.
18. Luthi, J.M.; Howald, H.; Claassen, H.; Rosler, K.; Vock, P.; Hoppeler, H. Structural changes in skeletal muscle tissue with heavy-resistance exercise. *Int J Sports Med* **1986**, *7*, 123-127, doi:10.1055/s-2008-1025748.
19. Tang, J.E.; Hartman, J.W.; Phillips, S.M. Increased muscle oxidative potential following resistance training induced fibre hypertrophy in young men. *Appl Physiol Nutr Metab* **2006**, *31*, 495-501, doi:10.1139/h06-026.
20. Mollenhauer, H.H. Artifacts caused by dehydration and epoxy embedding in transmission electron microscopy. *Microsc Res Tech* **1993**, *26*, 496-512, doi:10.1002/jemt.1070260604.
21. Rasch, A.; Bystrom, A.H.; Dalen, N.; Berg, H.E. Reduced muscle radiological density, cross-sectional area, and strength of major hip and knee muscles in 22 patients with hip osteoarthritis. *Acta Orthop* **2007**, *78*, 505-510, doi:10.1080/17453670710014158.
22. Lamb, D.A.; Moore, J.H.; Smith, M.A.; Vann, C.G.; Osburn, S.C.; Ruple, B.A.; Fox, C.D.; Smith, K.S.; Altonji, O.M.; Power, Z.M., et al. The effects of resistance training with or without peanut protein supplementation on skeletal muscle and strength adaptations in older individuals. *J Int Soc Sports Nutr* **2020**, *17*, 66, doi:10.1186/s12970-020-00397-y.
23. Alway, S.E.; MacDougall, J.D.; Sale, D.G.; Sutton, J.R.; McComas, A.J. Functional and structural adaptations in skeletal muscle of trained athletes. *J Appl Physiol (1985)* **1988**, *64*, 1114-1120, doi:10.1152/jappl.1988.64.3.1114.
24. Scarpulla, R.C.; Vega, R.B.; Kelly, D.P. Transcriptional integration of mitochondrial biogenesis. *Trends Endocrinol Metab* **2012**, *23*, 459-466, doi:10.1016/j.tem.2012.06.006.
25. Larsen, S.; Nielsen, J.; Hansen, C.N.; Nielsen, L.B.; Wibrand, F.; Stride, N.; Schroder, H.D.; Boushel, R.; Helge, J.W.; Dela, F., et al. Biomarkers of mitochondrial content in skeletal muscle of healthy young human subjects. *J Physiol* **2012**, *590*, 3349-3360, doi:10.1113/jphysiol.2012.230185.
26. Glancy, B.; Balaban, R.S. Energy Metabolism Design of the Striated Muscle Cell. *Physiol Rev* **2021**, 10.1152/physrev.00040.2020, doi:10.1152/physrev.00040.2020.
27. Glancy, B.; Hartnell, L.M.; Malide, D.; Yu, Z.X.; Combs, C.A.; Connelly, P.S.; Subramaniam, S.; Balaban, R.S. Mitochondrial reticulum for cellular energy distribution in muscle. *Nature* **2015**, *523*, 617-620, doi:10.1038/nature14614.

28. Willingham, T.B.; Kim, Y.; Lindberg, E.; Bleck, C.K.E.; Glancy, B. The unified myofibrillar matrix for force generation in muscle. *Nat Commun* **2020**, *11*, 3722, doi:10.1038/s41467-020-17579-6.
29. *Essentials of Stregnth Training and Conditioning*. 4 ed.; Haff, G.G.; Triplett, N.T., Eds.; Human Kinetics: Champaign, IL, 2016.
30. Mobley, C.B.; Haun, C.T.; Roberson, P.A.; Mumford, P.W.; Romero, M.A.; Kephart, W.C.; Anderson, R.G.; Vann, C.G.; Osburn, S.C.; Pledge, C.D., et al. Effects of Whey, Soy or Leucine Supplementation with 12 Weeks of Resistance Training on Strength, Body Composition, and Skeletal Muscle and Adipose Tissue Histological Attributes in College-Aged Males. *Nutrients* **2017**, *9*, doi:10.3390/nu9090972.
31. American College of Sports, M.; Sawka, M.N.; Burke, L.M.; Eichner, E.R.; Maughan, R.J.; Montain, S.J.; Stachenfeld, N.S. American College of Sports Medicine position stand. Exercise and fluid replacement. *Med Sci Sports Exerc* **2007**, *39*, 377-390, doi:10.1249/mss.0b013e31802ca597.
32. Evans, W.J.; Phinney, S.D.; Young, V.R. Suction applied to a muscle biopsy maximizes sample size. *Med Sci Sports Exerc* **1982**, *14*, 101-102.
33. Roberts, M.D.; Young, K.C.; Fox, C.D.; Vann, C.G.; Roberson, P.A.; Osburn, S.C.; Moore, J.H.; Mumford, P.W.; Romero, M.A.; Beck, D.T., et al. An optimized procedure for isolation of rodent and human skeletal muscle sarcoplasmic and myofibrillar proteins. *J Biol Methods* **2020**, *7*, e127, doi:10.14440/jbm.2020.307.
34. Cohen, S.; Brault, J.J.; Gygi, S.P.; Glass, D.J.; Valenzuela, D.M.; Gartner, C.; Latres, E.; Goldberg, A.L. During muscle atrophy, thick, but not thin, filament components are degraded by MuRF1-dependent ubiquitylation. *J Cell Biol* **2009**, *185*, 1083-1095, doi:10.1083/jcb.200901052.
35. Vann, C.G.; Osburn, S.C.; Mumford, P.W.; Roberson, P.A.; Fox, C.D.; Sexton, C.L.; Johnson, M.R.; Johnson, J.S.; Shake, J.; Moore, J.H., et al. Skeletal Muscle Protein Composition Adaptations to 10 Weeks of High-Load Resistance Training in Previously-Trained Males. *Front Physiol* **2020**, *11*, 259, doi:10.3389/fphys.2020.00259.
36. Wen, Y.; Murach, K.A.; Vechetti, I.J., Jr.; Fry, C.S.; Vickery, C.; Peterson, C.A.; McCarthy, J.J.; Campbell, K.S. MyoVision: software for automated high-content analysis of skeletal muscle immunohistochemistry. *J Appl Physiol (1985)* **2018**, *124*, 40-51, doi:10.1152/japplphysiol.00762.2017.
37. Duddy, W.; Duguez, S.; Johnston, H.; Cohen, T.V.; Phadke, A.; Gordish-Dressman, H.; Nagaraju, K.; Gnocchi, V.; Low, S.; Partridge, T. Muscular dystrophy in the mdx mouse is a severe myopathy compounded by hypotrophy, hypertrophy and hyperplasia. *Skelet Muscle* **2015**, *5*, 16, doi:10.1186/s13395-015-0041-y.
38. Gokhin, D.S.; Ward, S.R.; Bremner, S.N.; Lieber, R.L. Quantitative analysis of neonatal skeletal muscle functional improvement in the mouse. *J Exp Biol* **2008**, *211*, 837-843, doi:10.1242/jeb.014340.
39. Kaldma, A.; Klepinin, A.; Chekulayev, V.; Mado, K.; Shevchuk, I.; Timohhina, N.; Tepp, K.; Kandashvili, M.; Varikmaa, M.; Koit, A., et al. An in situ study of bioenergetic properties of human colorectal cancer: the regulation of mitochondrial respiration and distribution of flux control among the components of ATP synthasome. *Int J Biochem Cell Biol* **2014**, *55*, 171-186, doi:10.1016/j.biocel.2014.09.004.
40. Mobley, C.B.; Mumford, P.W.; Kephart, W.C.; Haun, C.T.; Holland, A.M.; Beck, D.T.; Martin, J.S.; Young, K.C.; Anderson, R.G.; Patel, R.K., et al. Aging in Rats Differentially

 doi:10.20944/preprints202106.0349.v1

Affects Markers of Transcriptional and Translational Capacity in Soleus and Plantaris Muscle. *Front Physiol* **2017**, *8*, 518, doi:10.3389/fphys.2017.00518.